

Can we learn where people come from?

Retracing of origins in merging situations

Marion Gödel*, Luca Spataro, Gerta Köster

Department of Computer Science and Mathematics,
Munich University of Applied Sciences
Department of Informatics, Technical University of Munich

December 22, 2020

Abstract

One crucial information for a pedestrian crowd simulation is the number of agents moving from an origin to a certain target. While this setup has a large impact on the simulation, it is in most setups challenging to find the number of agents that should be spawned at a source in the simulation. Often, number are chosen based on surveys and experience of modelers and event organizers. These approaches are important and useful but reach their limits when we want to perform real-time predictions. In this case, a static information about the inflow is not sufficient. Instead, we need a dynamic information that can be retrieved each time the prediction is started. Nowadays, sensor data such as video footage or GPS tracks of a crowd are often available. If we can estimate the number of pedestrians who stem from a certain origin from this sensor data, we can dynamically initialize the simulation. In this study, we use density heatmaps that can be derived from sensor data as input for a random forest regressor to predict the origin distributions. We study three different datasets: A simulated dataset, experimental data, and a hybrid approach with both experimental and simulated data. In the hybrid setup, the model is trained with simulated data and then tested on experimental data. The results demonstrate that the random forest model is able to predict the origin distribution based on a single density heatmap for all three configurations. This is especially promising for applying the approach on real data since there is often only a limited amount of data available.

*Corresponding author: marion.goedel@hm.edu

1 Introduction

One crucial initial condition for a pedestrian crowd simulation is the number of agents moving from an origin to a certain target. This setting has a high impact on the simulation result. At the same time, it is in most setups challenging to find the number of agents that should be generated at a source in the simulation. Often, number are chosen based on surveys and experience of modelers and event organizers. These approaches are important and useful but reach their limits when we want to perform real-time predictions. In this case, a static information about the inflow is not sufficient. Instead, we need an updated information each time the prediction is calculated. We want to use available sensor data of the pedestrians currently present in an observation area to estimate the number of pedestrians who stem from a certain origin. This can serve as an approximation of the number of pedestrians entering the scenario at this origin for the next prediction. As sensors often video cameras are present on site of urban events. Outside of controlled experiments, it is highly challenging to estimate the trajectories of single pedestrians from the video footage. Nevertheless, there are several approaches to estimate the current density from video footage. Consequently, we use density heatmaps as input for this study.

1.1 Research question

Can we use machine learning methods to estimate the distributions of pedestrians on the origins based on a single density heatmap?

1.2 Background

In previous work, we were able to demonstrate that it is possible to prediction direction distributions at crossing based on simulated data with an accuracy about 80% as a proof-of-concept [2]. Now, we want to test the methodology on data of pedestrians as e.g., surveillance data, experimental data, or similar. We need trajectories to create the heatmaps and for the response, the actual distributions of the origins. Unfortunately, there are only a few public data sets of pedestrian trajectories available. In particular, to our knowledge there is no public dataset of a crossing scenario with unidirectional flow available. There are, on the other hand, several datasets on merging behavior of pedestrians. Therefore, we decided to test our routines with simulated and experimental data on a merging scenario. In this setup, the distribution on the destination is trivial since everyone heads to the same target. Nevertheless, it is interesting to study if we can find out from which origins pedestrians come. We hope that the problems are similar enough that if the retracing of the pedestrians to the origin distributions is successful, the prediction of the target distributions is also successful on real data. In both cases, the available input data are density heatmaps and we are trying to infer the percentage of pedestrians coming from or heading to a known list of origins or destinations, respectively.

2 Methods and materials

We choose the T-Junction experiments from [1, 8] as scenario. The trajectories as well as video footage of the experiment are available online ¹.

2.1 Simulation setup

All simulations are carried out with the Optimal Steps Model [5, 7] of the open-source simulation framework Vadere [3]. We performed a manual calibration of the parameters to the experimental data. In particular, the navigation field was adapted to the data. It is calculated with obstacles method with factor `obstacleDensityWeight` = 0.3. That means that the obstacles are regarded in particular way in the calculation of the navigation field. As a result, agents keep more distance to the walls. For the comparison of simulated and experimental data, we used the measurement areas defined in [1].

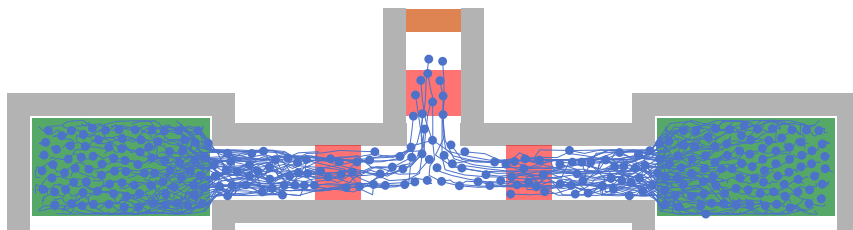
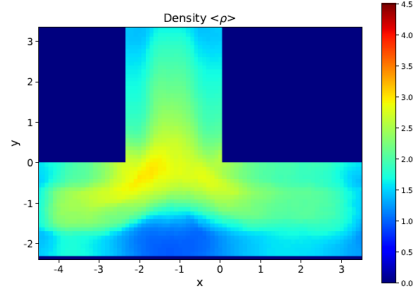


Figure 1: Snapshot of the simulation with Vadere. Agents are moving from two origins (green) to one destination (orange) through a T-junction setup. Measurement areas are shown in red.

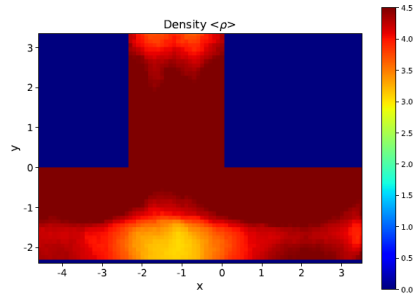
2.1.1 Calibration of the simulation: navigation field

The Voronoi diagrams are calculated with the package `spatial` of the Python library `scipy` [6].

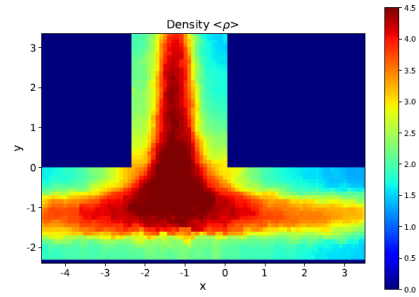
¹<https://doi.org/10.34735/ped.2009.7>



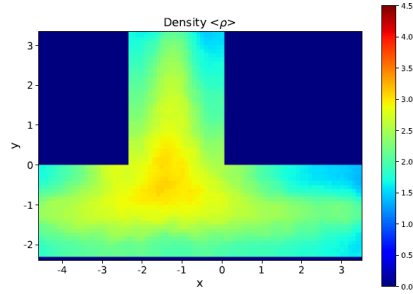
(a) Experimental data set.



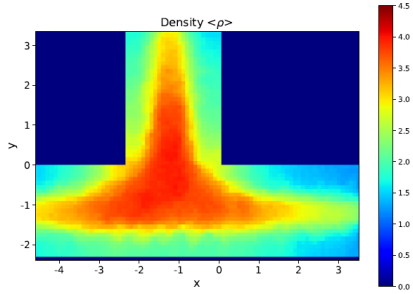
(b) Simulated data set: static floor field.



(c) Simulated data set: dynamic floor field.



(d) Simulated data set: static floor field with obstacle density 0.3.



(e) Simulated data set: static floor field with obstacle density 0.9.

Figure 2: Average Voronoi density for the experimental data set (a) compared to the simulation with 4 different navigation fields (b-e).

We found the best agreement between simulated data and the experimental data for the static floor field with obstacle density with factor 0.3. For the following simulations, this configuration is used.

2.1.2 Calculation density heatmaps

Analogue to [2], the density heatmaps are calculated from the pedestrian trajectories with a Gaussian density function [5].

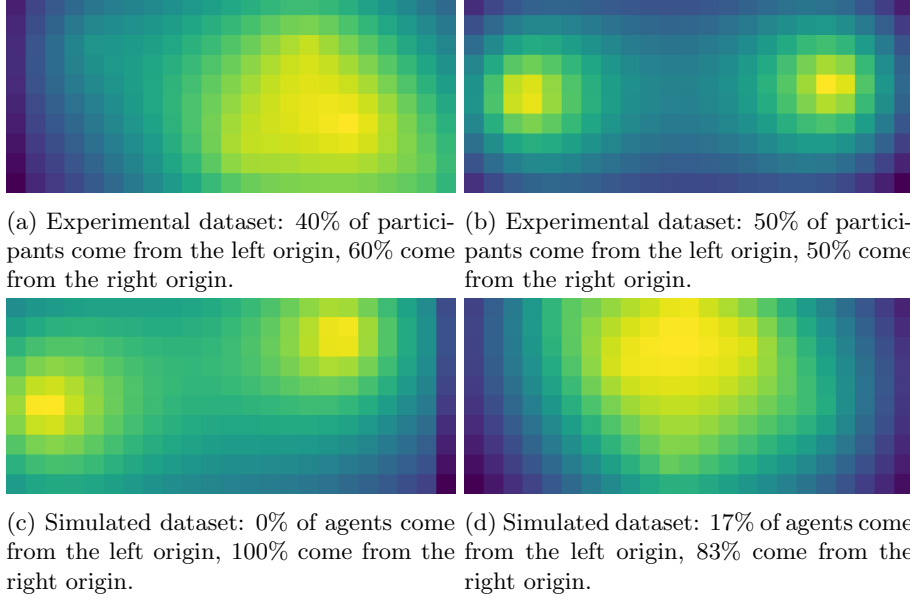


Figure 3: Exemplary density heatmaps for both experimental and simulated datasets.

2.1.3 Comparison of simulation and experiment

We compare the obtained simulated data with the experimental dataset. In Figure 4, the trajectories for two configurations (entrance widths $0.5m$ and $2.4m$) are compared. We observe that the agent flows / trajectories from left and right origin are more mixed in the simulation compared to the pedestrian trajectories from the experiment. For the experimental data, we observe an area free of pedestrians below the corridor. This effect is stronger for smaller entrance widths. We can mainly observe the effect in the experimental data set, only slightly in the simulated data.

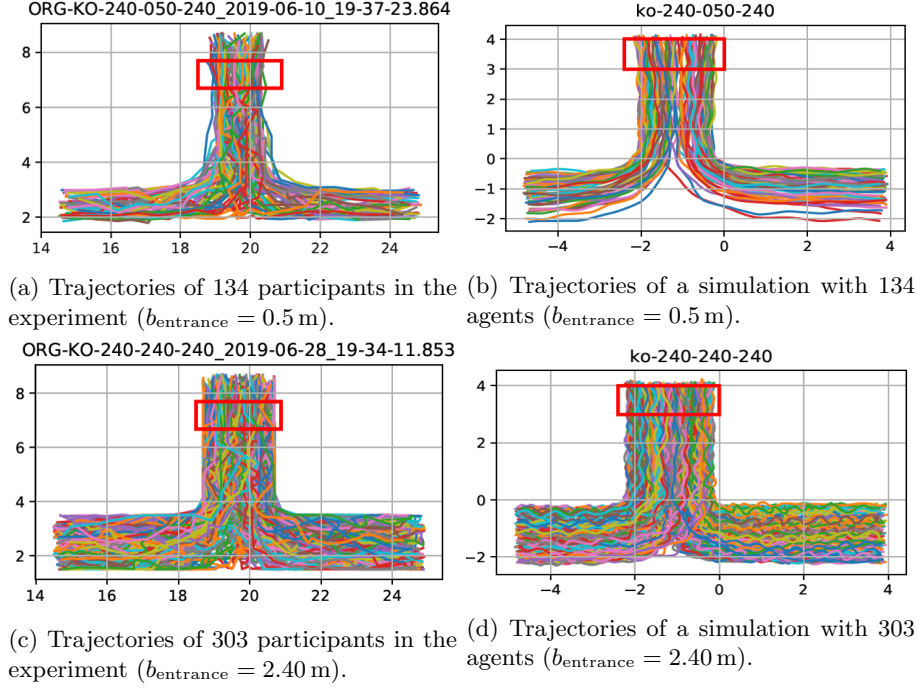


Figure 4: Comparison of trajectories between experiment and simulation.

In addition, we show the fundamental diagrams for the simulated data. It can be compared to the results from the experiment in [8]. In Figure 5, the density-speed relationship is evaluated for the three measurement areas defined in [1] that are depicted in red in Figure 1.

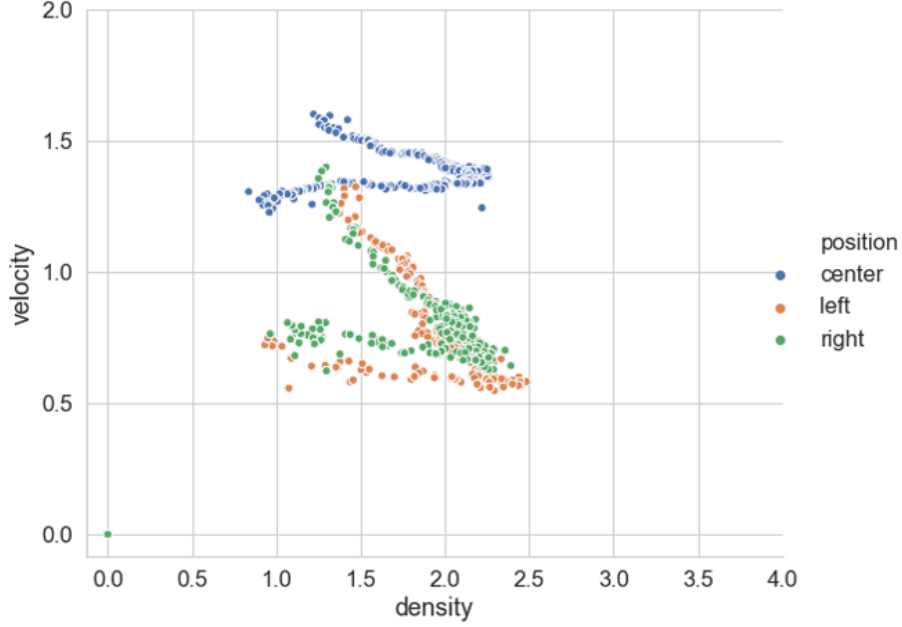


Figure 5: Fundamental diagrams for simulated data in the T-junction setup. The simulation was set up according to the experiment in [8] with 303 agents and an entrance width of 2.4 m .

2.1.4 Simulated dataset

Our simulated data set consists of three simulation runs for each of the seven scenarios (240-50-240, 240-60-240, 240-80-240, 240-100-240, 240-120-240, 240-150-240, 240-240-240), analogue to [1]. The tuple of numbers refers to the size of the entrance of the waiting area b_{entrance} , the width of the corridor b_{cor1} and the width of the corridor towards the exit b_{exit} . In total, we obtain 14.714 samples from the simulations.

Due to the functional whiteness of the simulator, we may have many identical density heatmaps. Since this increases the noise in the relationship between input and output, we decided to throw out identical consecutive heatmaps.

After removing duplicates, we end up with 7.895 heatmaps. When looking closer at Table 1, we notice the heatmaps are not equally distributed between the existing origin distributions and the majority of heatmaps correspond to a 50% | 50% distribution. To prevent the random forest model to only predicts 50% | 50%, we reduce the number of heatmaps for the equal case, see Table 2. In the end, 7.023 heatmaps remain.

Table 1: Origin distributions in full dataset. Table 2: Origin distributions in reduced dataset.

Left	Right	# Heatmaps	Left	Right	# Heatmaps
0.000000	1.000000	557	0.000000	1.000000	557
0.125000	0.875000	2	0.125000	0.875000	2
0.142857	0.857143	7	0.142857	0.857143	7
0.166667	0.833333	70	0.166667	0.833333	70
0.200000	0.800000	245	0.200000	0.800000	245
0.222222	0.777778	1	0.222222	0.777778	1
0.250000	0.750000	444	0.250000	0.750000	444
0.285714	0.714286	64	0.285714	0.714286	64
0.333333	0.666667	853	0.333333	0.666667	853
0.375000	0.625000	23	0.375000	0.625000	23
0.400000	0.600000	592	0.400000	0.600000	592
0.428571	0.571429	154	0.428571	0.571429	154
0.444444	0.555556	3	0.444444	0.555556	3
0.500000	0.500000	1759	0.500000	0.500000	887
0.555556	0.444444	4	0.555556	0.444444	4
0.571429	0.428571	111	0.571429	0.428571	111
0.600000	0.400000	652	0.600000	0.400000	652
0.625000	0.375000	22	0.625000	0.375000	22
0.666667	0.333333	931	0.666667	0.333333	931
0.714286	0.285714	54	0.714286	0.285714	54
0.750000	0.250000	469	0.750000	0.250000	469
0.800000	0.200000	220	0.800000	0.200000	220
0.833333	0.166667	57	0.833333	0.166667	57
0.857143	0.142857	11	0.857143	0.142857	11
0.875000	0.125000	4	0.875000	0.125000	4
1.000000	0.000000	586	1.000000	0.000000	586

2.2 Random forest

We decided to use random forest as machine learning model as in [2]. It is an easy and robust algorithm that needs only a few parameters and often provides good results. Consequently, the configuration is easy, and the model can be used right away. In addition, the model is robust on the parameters which is not necessarily the case for machine learning models. Furthermore, the output is interpretable.

The input to our random forest routine is a single density heatmap, generated as described before, from pedestrian positions using a Gaussian function. We want to predict the percentage of pedestrians stemming from each of the two origins from the density heatmap.

For the random forest we use the `RandomForestRegressor` from the Python

library scikit-learn [4]. Before training, we shuffle the heatmaps and divide them into training and test sets with 80% and 20% respectively. For each origin, we train one forest with 50 trees. Consequently, when evaluating the model, each origin is also predicted separately, and the predictions are normalized over both directions to assure that they sum up to 100%.

3 Results and discussion

Now, we use our Random forest setup to predict the origin distributions from density heatmaps. We use three different data set: First, the dataset that contains simulations performed with Vadere. Second, the experimental dataset calculated from the trajectory data. Third, a hybrid dataset where we train the random forest with simulated data but evaluate its performance on the experimental data. For each setup, we perform five runs to study the variation in the results.

3.1 Performance measure

The random forest routines can provide an out of bag error estimate as well as the coefficient of determination. However, both quantities are applied before the model predictions are normalized. Therefore, we split our dataset into a training and a test set and compare the prediction on the test set to the corresponding response to evaluate the model. In a first step, we evaluate the Euclidean norm of the difference vector. In the second step, we derive a relative error. Since we normalize the prediction, the maximum error

$$e_{max} = \sqrt{2 \cdot 100^2} \approx 141.42 \quad (1)$$

occurs if we predict that all pedestrians within the cutout head left while, in fact, they head right (or straight). The relative error is then

$$e = 100 \cdot \frac{y - \hat{y}}{e_{max}}, \quad (2)$$

where y is the response on the test set and \hat{y} is the prediction on the test set. Thereby we obtain a relative error of the prediction that is easy to interpret. Thus, the relative error is used as a measure.

3.2 Retracing using simulated data

For the first setup, we train and test the random forest solely on simulated data. We generate simulation data for all distributions of pedestrians on the origins. We expect an accuracy of roughly 80%, similar to our observations in [2] where we predicted the target distributions. The results in Table 3 show an accuracy of about 80% of the setup with a standard deviation of about 15%.

Table 3: Relative error of random forest prediction using simulated data (7.023 density heatmaps).

	Run 1	Run 2	Run 3	Run 4	Run 5
Mean Euclidean error	19.23%	20.15%	19.85%	19.78%	19.57%
Stdev Euclidean error	14.98%	15.08%	15.93%	15.47%	15.29%

3.3 Retracing using experimental data

In this section, we analyze the results of the random forest prediction based on experimental data. The dataset from the experiments shows only a few different distributions of the pedestrians on the origins. In experimental data set, mainly an equal distribution of the pedestrians on the origins is observed. We mainly observe the following distributions: 100 | 0, 50 | 50, 66 | 34, 75 | 25. This is a consequence of the experimental setup and the size of the observation area. Table 4 summarizes the results for the experimental dataset for both training and evaluation. The prediction accuracy is lower than when we used solely simulated data. We observe that the equal distribution is estimated well, due to the large data base. Other distributions are estimated with lower accuracy. Most of the predicted distributions are targets from the training set even though we use a regressor, not a classifier.

Table 4: Relative error of random forest prediction using the experiment data (6.678 density heatmaps).

	Run 1	Run 2	Run 3	Run 4	Run 5
Mean Euclidean error	11.12%	9.68%	9.66%	10.33%	9.82%
Stdev Euclidean error	15.89%	13.46%	13.19%	14.48%	13.89%

3.4 Retracing using hybrid approach

We observed that the available experimental data has only a few different distributions. Unfortunately, performing experiments is expensive, time-consuming, and complicated. Ideally, we would have a heterogeneous set of participants to reflect the average population well. In addition, results may strongly depend on the setup, how the subjects are primed, if and how subjects know each other, their form of the day and many more. In addition, the culture may have an impact on the behavior, so we need comparable studies.

Simulated data on the other hand can be generated easily and cheap. For applications, none or only limited experimental data is available.

As a result, we decided to complement the experimental data with simulated data: The algorithm is trained solely on simulated data. The testing is performed in two steps: First, testing of the trained random forest on the simulated data. This aims to find out how well the forest is trained. The results

should be identical to Section 3.2. Second, testing of the trained random forest on the experimental data. The goal of this part is to find out if the gained knowledge from the simulations can be extrapolated to real data.

Table 5 lists the results for 5 trainings of the random forest algorithm. As the input data is shuffled, the separation in training and test data varies among the runs. We observe a mean error about 30% with a standard deviation of approximately 25%. As expected, the results are inferior to training and testing with the same data set. Both the size of the error and the size of the standard deviation have almost doubled. Nevertheless, we still obtain an accuracy of about 70%. That means, it is possible to train with simulated data and use the trained forest for predictions on experimental data.

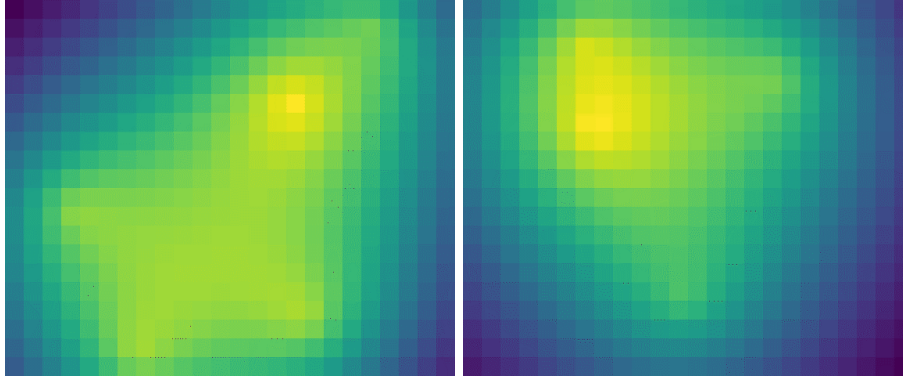
Table 5: Relative error of random forest prediction using the hybrid dataset.

	Run 1	Run 2	Run 3	Run 4	Run 5
Mean Euclidean error	29.36%	29.39%	29.24%	29.43%	29.40%
Stdev Euclidean error	24.48%	24.73%	24.51%	24.70%	24.80%

4 Extending the observation area

In the previous chapters, we saw limitations of the results due to the low variation of the origin distributions present in the data sets. Therefore, we decided to use a larger observation area so that more than a maximum of two pedestrians can be present at one time. That allows a larger variation in the distributions on the origins. The new observation area has the size of $2.4\text{ m} \times 2\text{ m}(B \times H)$. It is again placed over the full corridor width just before the target.

In Figure 6, we depicted two exemplary heatmaps for the larger observation area. Due to the larger observation area (2), more variation in the data is seen. Nevertheless, the equal distribution on both origins (50% | 50%) and distributions close to it are still most common.



(a) Experimental dataset: 60% of participants come from the left origin, 40% come from the right origin. (b) Simulated dataset: 25% of agents come from the left origin, 75% come from the right origin.

Figure 6: Exemplary density heatmaps for the larger observation area (#2).

In Tables 6, 7, 8 the results for the random forest prediction of the origin distributions are shown for solely simulated data, solely experimental data, and the hybrid dataset with simulated data for training and experimental data for testing, respectively. The results for all datasets have improved compared to the smaller observation area (#1). The improvement can be seen from a decrease in the mean error in combination with a decrease of the standard deviation. That means, that there is less variation of the quality of the prediction within the test set.

Table 6: Relative error of random forest prediction using simulated data generated with Vadere (observation area #2, 9.666 samples).

	Run 1	Run 2	Run 3	Run 4	Run 5
Mean Euclidean error	12.02%	12.03%	12.09%	11.61%	11.82%
Stdev Euclidean error	9.64%	10.07%	9.82%	9.56%	9.39%

Table 7: Relative error of random forest prediction using experiment data (observation area #2, 7.221 samples).

	Run 1	Run 2	Run 3	Run 4	Run 5
Mean Euclidean error	7.65%	7.63%	7.70%	7.85%	8.02%
Stdev Euclidean error	9.33%	9.27%	8.37%	8.88%	9.55%

Table 8: Relative error of random forest prediction using the hybrid dataset (observation area #2).

	Run 1	Run 2	Run 3	Run 4	Run 5
Mean Euclidean error	19.78%	19.65%	19.67%	19.80%	19.56%
Stdev Euclidean error	18.63%	18.42%	18.31%	18.77%	18.15%

5 Conclusion and outlook

We were able to retrace the origin distributions based on single density heatmap. Basis of this study was a merging experiment (T-junction) where two pedestrian streams head for the same destination. We trained as random forest regressor with three different data sets: The first data set stems from simulations with the simulation framework Vadere. The setup of the simulation resembles the T-junction experiment. The second dataset is the publicly available data of the experiment. The last dataset is a hybrid dataset of both sources that means we used simulated data for training the random forest and experimental data for testing.

We observed the best results ($\approx 92\%$) on experimental data which is most likely due to the limited set of origin distributions in the data set. The accuracy of the random forest model on simulated data was at about 88%. Finally, the hybrid approach yielded an accuracy of approximately 80%. This is a promising result that motivates the application of the approach on real data. Especially for applications, we believe the results of the hybrid approach are encouraging because often there will not be enough training data available.

In the future, we would like to look into other scenarios and topographies more complicated than the one studied here. Unfortunately, there is only limited amount of public data available. In addition, we want to try other learning models to see how they perform on the problem, in particular convolutional neural networks that are designed to work on image data. Furthermore, we believe that for more complicated scenarios, it will be beneficial or maybe even necessary to consider a time-dependent input, that is a time series of consecutive heatmaps.

Funding: This research was funded by the German Federal Ministry of Education and Research (BMBF) grant number 13N14464 (S2UCRE).

A Origin distributions observed in different datasets (simulated data, experimental data) for both observation areas (1,2)

Table 9: Origin distributions in experiment dataset using observation area #1
($2.4\,m \times 1\,m$).

	Left	Right	#Frames
0	0.000000	1.000000	1372
1	0.166667	0.833333	11
2	0.200000	0.800000	45
3	0.250000	0.750000	294
4	0.285714	0.714286	3
5	0.333333	0.666667	881
6	0.400000	0.600000	517
7	0.428571	0.571429	20
8	0.500000	0.500000	2241
9	0.571429	0.428571	23
10	0.600000	0.400000	471
11	0.625000	0.375000	2
12	0.666667	0.333333	838
13	0.714286	0.285714	2
14	0.750000	0.250000	304
15	0.800000	0.200000	35
16	1.000000	0.000000	738

Table 10: Origin distributions in experiment dataset using observation area #2 ($2.4\text{ m} \times 2\text{ m}$).

	Left	Right	#Frames
0	0.000000	1.000000	873
1	0.125000	0.875000	1
2	0.142857	0.857143	6
3	0.166667	0.833333	16
4	0.200000	0.800000	45
5	0.222222	0.777778	15
6	0.250000	0.750000	166
7	0.285714	0.714286	164
8	0.300000	0.700000	25
9	0.333333	0.666667	471
10	0.363636	0.636364	62
11	0.375000	0.625000	347
12	0.400000	0.600000	458
13	0.416667	0.583333	22
14	0.428571	0.571429	473
15	0.444444	0.555556	478
16	0.454545	0.545455	81
17	0.461538	0.538462	1
18	0.500000	0.500000	829
19	0.538462	0.461538	1
20	0.545455	0.454545	76
21	0.555556	0.444444	381
22	0.571429	0.428571	386
23	0.583333	0.416667	22
24	0.600000	0.400000	461
25	0.615385	0.384615	8
26	0.625000	0.375000	200
27	0.636364	0.363636	38
28	0.666667	0.333333	504
29	0.700000	0.300000	20
30	0.714286	0.285714	55
31	0.750000	0.250000	221
32	0.777778	0.222222	1
33	0.800000	0.200000	72
34	0.833333	0.166667	27
35	1.000000	0.000000	215

Table 11: Origin distributions observed in simulated dataset using observation area #1 ($2.4\text{ m} \times 1\text{ m}$).

	Left	Right	#Frames
0	0.000000	1.000000	557
1	0.125000	0.875000	2
2	0.142857	0.857143	7
3	0.166667	0.833333	70
4	0.200000	0.800000	245
5	0.222222	0.777778	1
6	0.250000	0.750000	444
7	0.285714	0.714286	64
8	0.333333	0.666667	853
9	0.375000	0.625000	23
10	0.400000	0.600000	592
11	0.428571	0.571429	154
12	0.444444	0.555556	3
13	0.500000	0.500000	887
14	0.555556	0.444444	4
15	0.571429	0.428571	111
16	0.600000	0.400000	652
17	0.625000	0.375000	22
18	0.666667	0.333333	931
19	0.714286	0.285714	54
20	0.750000	0.250000	469
21	0.800000	0.200000	220
22	0.833333	0.166667	57
23	0.857143	0.142857	11
24	0.875000	0.125000	4
25	1.000000	0.000000	586

Table 12: Origin distributions in simulated dataset using observation area #2 ($2.4\text{ m} \times 2\text{ m}$).

	Left	Right	#Frames		Left	Right	#Frames
0	0.000000	1.000000	70	28	0.470588	0.529412	2
1	0.100000	0.900000	5	29	0.500000	0.500000	920
2	0.111111	0.888889	6	30	0.533333	0.466667	17
3	0.125000	0.875000	14	31	0.538462	0.461538	187
4	0.142857	0.857143	14	32	0.545455	0.454545	383
5	0.166667	0.833333	67	33	0.555556	0.444444	285
6	0.181818	0.818182	18	34	0.562500	0.437500	3
7	0.200000	0.800000	89	35	0.571429	0.428571	482
8	0.222222	0.777778	45	36	0.583333	0.416667	270
9	0.230769	0.769231	6	37	0.600000	0.400000	548
10	0.250000	0.750000	179	38	0.615385	0.384615	133
11	0.272727	0.727273	79	39	0.625000	0.375000	264
12	0.285714	0.714286	122	40	0.636364	0.363636	204
13	0.300000	0.700000	126	41	0.642857	0.357143	36
14	0.307692	0.692308	31	42	0.666667	0.333333	594
15	0.333333	0.666667	565	43	0.692308	0.307692	31
16	0.357143	0.642857	37	44	0.700000	0.300000	98
17	0.363636	0.636364	237	45	0.714286	0.285714	178
18	0.375000	0.625000	246	46	0.727273	0.272727	64
19	0.384615	0.615385	138	47	0.733333	0.266667	1
20	0.400000	0.600000	612	48	0.750000	0.250000	185
21	0.416667	0.583333	295	49	0.769231	0.230769	4
22	0.428571	0.571429	431	50	0.777778	0.222222	35
23	0.437500	0.562500	3	51	0.800000	0.200000	102
24	0.444444	0.555556	326	52	0.833333	0.166667	93
25	0.454545	0.545455	405	53	0.857143	0.142857	39
26	0.461538	0.538462	228	54	0.875000	0.125000	8
27	0.466667	0.533333	23	55	0.888889	0.111111	2
28	0.470588	0.529412	2	56	1.000000	0.000000	81

References

- [1] Maik Boltes, Jun Zhang, Armin Seyfried, and Bernhard Steffen. T-junction: Experiments, trajectory collection, and analysis. In *2011 IEEE International Conference on Computer Vision Workshops (ICCV Workshops)*, pages 158–165, 11 2011.
- [2] Marion Gödel, Gerta Köster, Daniel Lehmberg, Manfred Gruber, Angelika Kneidl, and Florian Sesser. Can we learn where people go? *Collective Dynamics*, 2020.
- [3] Benedikt Kleinmeier, Benedikt Zönnchen, Marion Gödel, and Gerta Köster. Vadere: An open-source simulation framework to promote interdisciplinary understanding. *Collective Dynamics*, 4, 2019.
- [4] Fabian Pedregosa, Gaël Varoquaux, Alexandre Gramfort, Vincent Michel, Bertrand Thirion, Olivier Grisel, Mathieu Blondel, Peter Prettenhofer, Ron Weiss, Vincent Dubourg, Jake Vanderplas, Alexandre Passos, David Cournapeau, Matthieu Brucher, Matthieu Perrot, and Édouard Duchesnay. Scikit-learn: Machine learning in Python. *Journal of Machine Learning Research*, 12:2825–2830, 2011.
- [5] Michael J. Seitz and Gerta Köster. Natural discretization of pedestrian movement in continuous space. *Physical Review E*, 86(4):046108, 2012.
- [6] Pauli Virtanen, Ralf Gommers, Travis E. Oliphant, Matt Haberland, Tyler Reddy, David Cournapeau, Evgeni Burovski, Pearu Peterson, Warren Weckesser, Jonathan Bright, Stéfan J. van der Walt, Matthew Brett, Joshua Wilson, K. Jarrod Millman, Nikolay Mayorov, Andrew R. J. Nelson, Eric Jones, Robert Kern, Eric Larson, C J Carey, İlhan Polat, Yu Feng, Eric W. Moore, Jake VanderPlas, Denis Laxalde, Josef Perktold, Robert Cimrman, Ian Henriksen, E. A. Quintero, Charles R. Harris, Anne M. Archibald, Antônio H. Ribeiro, Fabian Pedregosa, Paul van Mulbregt, and SciPy 1.0 Contributors. SciPy 1.0: Fundamental Algorithms for Scientific Computing in Python. *Nature Methods*, 17:261–272, 2020.
- [7] Isabella von Sivers and Gerta Köster. Dynamic stride length adaptation according to utility and personal space. *Transportation Research Part B: Methodological*, 74:104–117, 2015.
- [8] Jun Zhang, Wolfram Klingsch, Andreas Schadschneider, and Armin Seyfried. Transitions in pedestrian fundamental diagrams of straight corridors and t-junctions. *Journal of Statistical Mechanics: Theory and Experiment*, 2011(06):P06004, 2011.